

# Optimized Digital Optical Switch Using Proton Exchanged Lithium Niobate Waveguides

G. Singh, R. P. Yadav, and V. Janyani

Department of Electronics and Communication Engineering

Malaviya National Institute of Technology Jaipur-India

[gschoudhary75@gmail.com](mailto:gschoudhary75@gmail.com)

**Abstract**— The main emphasis in developing DOS has been on achieving low crosstalk (CT). CT in the order of -30 dB is acceptable in conventional DOS and below that value is hard to achieve. Relatively low drive voltage (or power requirements) is also necessary to optimized DOS. This paper depicts the design of Y-branched digital optical switches (DOS) with optimized on-chip area coverage, reduced driving voltage and cross talk. The proposed switch is designed using channel profile of proton exchanged lithium niobate substrate. The electro-optic effect of the material has been investigated from the DOS operation.

**KEYWORDS:** Digital optical switch, electro optic effect, crystal cut, proton exchanged lithium niobate.

## I. INTRODUCTION

Use of all optical switches becoming popular with flexible fiber networks; in such types of systems, switching techniques find wide applications for network protection and reconfiguration, all optical networking -circuit switching and all optical networks. There are various optical switches like thermo optic, MEMS, bubble switch, integrated optic or electro-optic, acousto-optic and semiconductor switches [1]. Amongst these the semiconductor switches are one of the promising optical switches with the advantages of switching time to be very short. The semiconductor switches can be categorized as interferometer Mach-Zehnder switch, directional couplers, digital optical switch (DOS), and semiconductor optical amplifiers. In the modern age of communication, digital optical switch (DOS) has experienced maximum attention due to its

unique characteristics of low polarization and low wavelength sensitivity. DOS has commonly been used as a space switching component [2] in multiple wavelength optical communication system application [3].

Several types of approaches have been taken in DOS research like developing DOS using silica on silicon, silicon resin, polymers [4], amorphous silicon, III-V semiconductors and Lithium Niobate [5] [6]. Optical multiple access networks require switches that are capable of routing very high data rate signals in optical domain regardless of the wavelength and coding system chosen. Though opto-mechanical switches exhibit extremely low loss, their switching speed is slow, typically 1-10 ms, resulting in a significant loss of data [7]. Electro-optic waveguide switches however are capable of switching at very high speeds and by careful design broadband optical switches or DOS which are insensitive to polarization can be produced that are compatible with existing fiber optic networks. Several ideas like two-angle linear branch, a linear branch with a modified coupling region, tapered overlap of electrodes and waveguides [8], and shaped branches[9] have been proposed to reduce drive voltage in the DOS in the expense of high crosstalk. In this work, we have proposed the architecture of a Y-branched digital optical switch using channel profile of proton exchange on the lithium niobate substrate. The DOS has been simulated for switching performance analysis, determination of optimum driving voltage and inquiry of feasibility of the DOS operation.

## II. Y-BRANCH DIGITAL OPTICAL SWITCHES

The symmetrical Y branch 1x2 digital optical switches can be designed using the x-cut and z-cut crystal of the substrate, while the signal is propagating in y direction in order to use the electro-optic coefficients. A conventional Y digital optical switch layout is shown in Fig. 1.a-b with both crystal cut, can be designed using a linear waveguide followed by the tapered waveguide followed by two linear waveguides. The Y switch acts as a power divider, while both branches of Y type digital optical switch are symmetrical and when there is no biasing is applied across the branches. On application of the biasing, one of the branches becomes electrically asymmetric due to the electro-optic effect. The light is guided to a branch which has a higher refractive index due to the electro-optic effect [10]. On reversing the asymmetry the light can be guided to the other branch. Thus the biasing across the respective branch plays a key role in the switching.

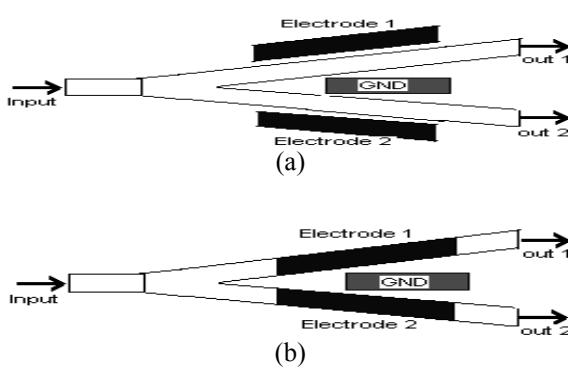


**Fig. 1** (a) X-cut DOS switch layout (b) Z-cut DOS switch layout [11].

The z-cut Y digital optical switch is designed under the electrodes as shown in Fig. 1.a. In z-cut substrate; the waveguide (TM mode used) suffers index change because of the vertical components of supplied electrical field. While, in x-cut substrate, waveguides are located between the center conductor and grounded electrodes as shown in Fig. 1.b. In this case, TE-mode optical signals are launched into the optical waveguide and the lateral component of the electrical field is used [11].

## III. DOS OPERATING PRINCIPLE BASED ON PROTON EXCHANGE IN $\text{LiNbO}_3$

Lithium Niobate crystal ( $\text{LiNbO}_3$ ) is most widely used electro-optic material in waveguides for DOS [12]. Proton exchange is one of the methods used for forming optical waveguides. Proton exchange in  $\text{LiNbO}_3$  involves a replacement of Lithium ions ( $\text{Li}^+$ ) by hydrogen ions, or protons ( $\text{H}^+$ ). The replacement causes a change in refractive index, thus forming a waveguide. The waveguide formation can have two stages:

- Basic proton exchange from an appropriate organic proton source when  $\text{LiNbO}_3$  substrate is immersed in the proton source, usually an acid melt, and heated for a couple of hours at temperatures ranging from 150-300 degrees Celsius.
- Annealing post processing involves solely heating of the sample to redistribute the Lithium and Hydrogen ions.

Proton exchange process on its own leads to a step-function index profile with a change of the refractive index [13]:

$$\Delta n_{es} = \beta \left[ 1 - \exp(-\gamma x^{\delta}) \right] \quad (1)$$

where the constants,  $\beta=0.1317$ ,  $\gamma=3.4576$ , and  $\delta=1.75$  are fitting parameters from experimental data, and  $x$  is the normalized  $\text{H}^+$  fractional concentration. The post-exchange annealing process leads to a different refractive distribution of the refractive index, which can be modeled as [13]:

$$n_e(y) = n_{e0} + \Delta n_{es} f(y) g(x) \quad (2)$$

where  $n_{e0}$  is the extraordinary bulk index of the  $\text{LiNbO}_3$  substrate,  $\Delta n_{es}$  is the maximum refractive index change on the surface, and  $f(y)$  and  $g(x)$  are the distribution functions. The waveguide depth after the exchange is obtained as [14]:

$$D_v = \sqrt{t D_0 \exp\left(-\frac{Q}{RT}\right)} \quad (3)$$

where  $t$  is the exchange process time,  $D_0$  is the diffusion constant of the proton exchange process,  $Q$  is the activation energy,  $T$  is the process temperature and  $R$  is the universal gas constant. The most common sources of Hydrogen ions  $H^+$  for proton exchange in  $LiNbO_3$  are the benzoic acid and the toluic acid [15] whose exchange parameters are shown in Table 1 [14].

TABLE 1 THE EXCHANGE PARAMETERS OF TOLUIC AND BENZOIC ACIDS [14]

Parameters	Toluic Acid	Benzoic Acid
Temperature range [°C]	109-263	122-249
Diffusion Constant $D_0$ [ $\mu\text{m}^2/\text{hr}$ ]	$7.02 \times 10^7$	$7.36 \times 10^9$
Activation energy $Q$ [kJ/mol]	75.58	94

### A. Device design and fabrication

The proposed Y-branch DOS structural architecture in the paper consists of one linear input waveguide of length 2500  $\mu\text{m}$  and width 8  $\mu\text{m}$ , a short central tapered region of length 500  $\mu\text{m}$  and tapering width ranging from 8  $\mu\text{m}$  to 16  $\mu\text{m}$  and two output linear waveguide arms of equal width of 8  $\mu\text{m}$  and equal length of 30000  $\mu\text{m}$ . The output waveguide arms are aligned to maintain a branching angle of 0.038 degree and central spacing of 20  $\mu\text{m}$  between the two output ports. The block diagram of the design is showed in Fig. 2.

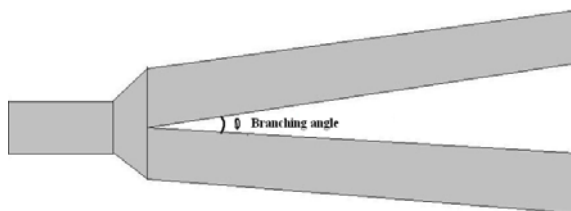


Fig. 2 Architecture of proposed Y-Branch DOS.

The lithium niobate DOS employed fabricated by the proton exchange from tuloic acid into an X-cut  $LiNbO_3$  substrate after 4 hours of exchange process at temperature of 280 degree Celsius. Normalized  $H^+$  fractional

concentration is kept at 0.5 with maximum refractive index change of 0.085 on the surface of the waveguide. Diffusion depth has been taken as 6.027  $\mu\text{m}$  and no annealing process has been applied.

The electrode regions have been applied with three sets of electrodes each of width 2  $\mu\text{m}$  and inter-electrode gaps for each pair of electrodes has been kept at 17  $\mu\text{m}$ , covering 3000  $\mu\text{m}$  of the DOS output arms. The electrode thickness has been taken as 1  $\mu\text{m}$  with no buffer layer due to x-cut configuration. The DOS architecture after insertion of electrode regions is shown in Fig. 3. Upon application of a switching voltage a step like optical response is achieved that is polarization independent and relatively wavelength insensitive. The wavelength range is constrained by the requirement that the input and output guides remain single mode.

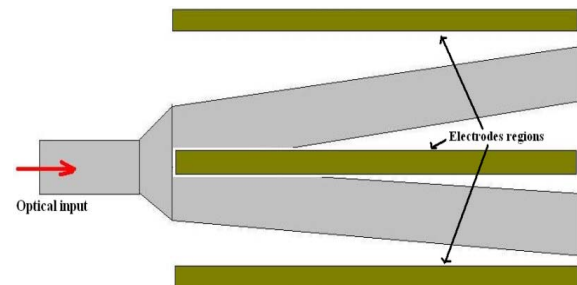
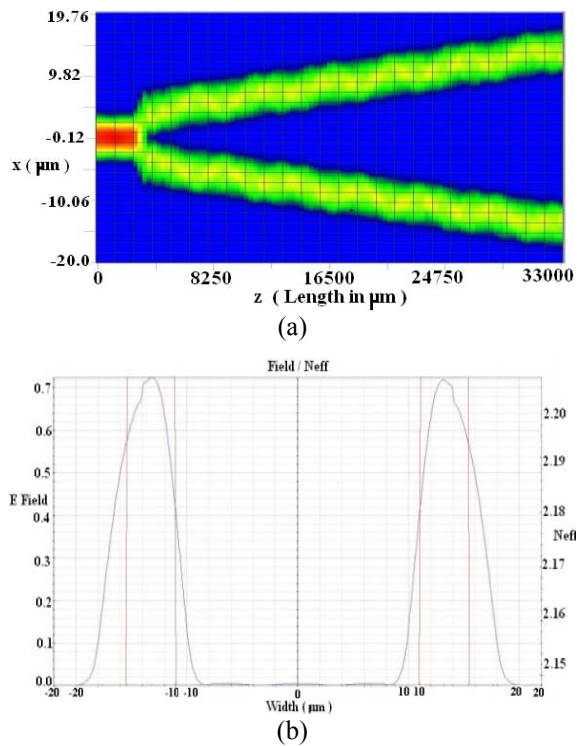


Fig. 3 Application of electrode region in the Y-branched DOS.

### IV. SIMULATION RESULTS

The proposed DOS has been simulated by finite difference beam propagating method, which investigates Lightwave propagation in axially varying waveguides. Design and 3D isotropic simulation results were done using OPTIBPM analyzer and simulator with VB scripting. When an input plane is generated in the input waveguide, the optical power traverses to the branching point and the perfect power dividing characteristic of the DOS was confirmed from the optical field intensity in the two output arms. Figures 3 and 4 show the simulation results for the Y-branched DOS

operating at different wavelengths of  $1.55\text{ }\mu\text{m}$ ,  $1.3\text{ }\mu\text{m}$  and  $0.83\text{ }\mu\text{m}$  respectively.



**Fig. 4** Operation at  $1.55\text{ }\mu\text{m}$  optical power input (a) Optical Field propagation in the DOS architecture (b) cut view of the output section, graph showing electric field intensity (curved shaped) and refractive index distribution (rectangular shaped) over the section.

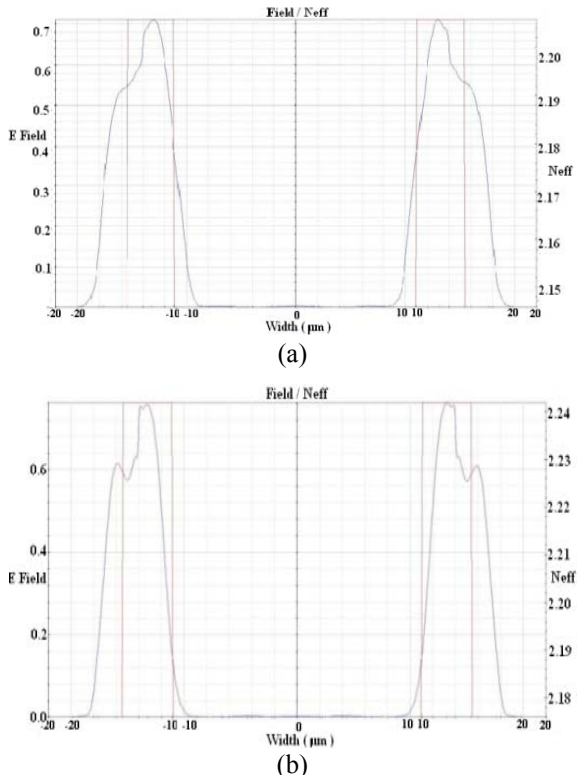


**Fig. 5** Cut-views of the output section, graph showing electric field intensity (curved shaped) and

refractive index distribution (rectangular shaped) over the section for DOS operation at (a)  $1.3\text{ }\mu\text{m}$ , and (b)  $0.83\text{ }\mu\text{m}$  optical power input without any voltage bias.

The comparison of Figs. 4 and 5 confirm the relatively low wavelength independence of the DOS operation. After the application of voltage bias in the middle electrode of the electrode region, we obtained switching response from the DOS. The driving voltage has found out to be 24 volts for most appropriate switching of input signal into one of the output ports depending on the bias of the voltage applied on the electrode. Figures 6 and 7 depicts the switching property of the proposed Y-branched DOS over application of positive and negative bias of 24 volts on the middle electrode inserted in the electrode region. We also observed that this bias voltage of 24 V as driving voltage has also brought relatively poor but feasible switching in case of different wavelength input signals of  $1.3\text{ }\mu\text{m}$  and  $0.83\text{ }\mu\text{m}$ .

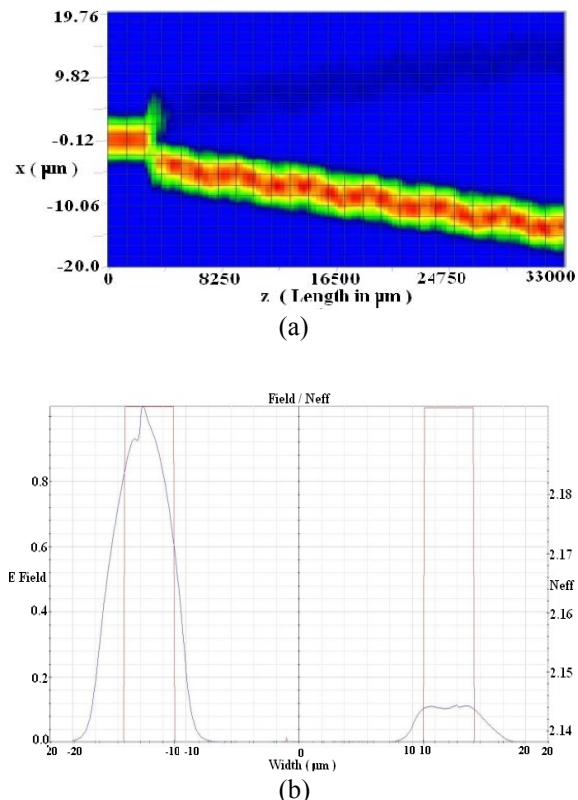


**Fig. 6** Operation at  $1.55\text{ }\mu\text{m}$  optical powers input with  $+24\text{ V}$  bias on middle electrode. (a) Optical field propagation in the DOS architecture (b) cut view of the output section, graph showing electric field intensity (curved shaped) and refractive index distribution (rectangular shaped) over the section.

The linear effect of voltage-length product of switch branches on crosstalk was kept in mind while measuring the crosstalk for different modes with different drive voltages. The minimum crosstalk levels obtained for the TM and the TE modes at a drive voltage of 24V (peak to peak) were -27dB and -32 dB, respectively. The crosstalk of the TE mode found to be ranged from -18 to -32dB and the crosstalk of the TM mode ranged from -19dB to -27dB for operating 1.5, 1.33 and 0.83 respectively. The insertion loss difference between the cross and the bar states was maintained less than 1.5dB in most simulated results.

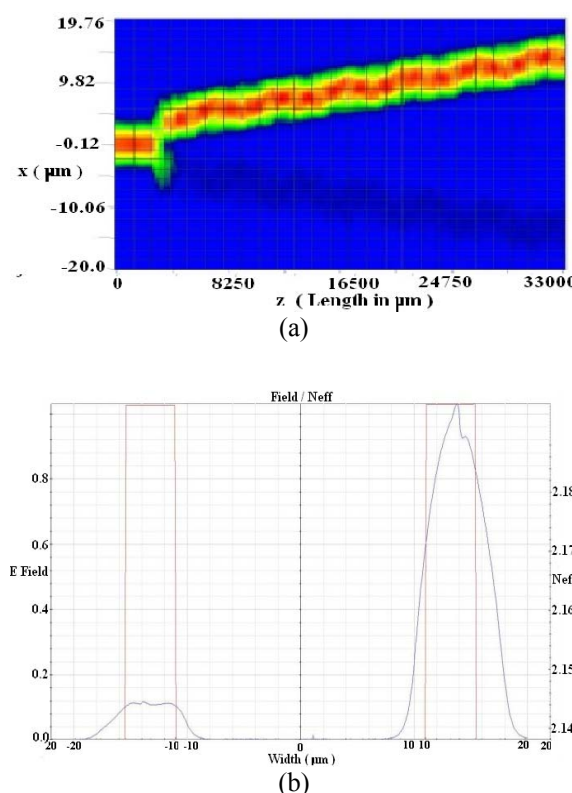


**Fig. 7** Operation at 1.55  $\mu\text{m}$  optical powers input with -24 V bias on middle electrode. (a) Optical field propagation in the DOS architecture (b) cut view of the output section, graph showing electric field intensity (curved shaped) and refractive index distribution (rectangular shaped) over the section.

The central electrode position and placing does introduce significant scattering loss particularly when overlap with near end of y-junction. A few hundred nanometers thick buffer layer of SO, SiO<sub>2</sub>, etc. can be used between the electrode and the waveguide to

avoid these losses and to provide more stable operation. Further optimization of electrodes like thickness, gaps between them and symmetry can also be done in order to reduce scattering losses.

## V. CONCLUSION

The Y-branched DOS proposed in the paper exhibits very low wavelength dependence in its switching operation. The driving voltage has been found out to be 24 V (peak to peak) which is feasible on-chip with the low crosstalk achieved ( -27dB and -32 dB for TM and TE modes respectively). The operation of the DOS at low attenuation operating wavelengths of 1.55  $\mu\text{m}$ , 1.3  $\mu\text{m}$  and 0.83  $\mu\text{m}$  has found out to be satisfactory. The future prospective of the work lies on varying the proton exchange parameters of the channel profile used in the DOS architecture and analyzing the respective reduction in driving voltage to optimize the switching performance.

## ACKNOWLEDGMENT

This work is dedicated to the Institutional excellence in optics research. We heartily thank to project TEQIP, MNIT for procurement of Optiwave simulator.

## REFERENCES

- [1] G. I. Papadimitriou, C. Papazoglou, and A. S. Pomportsis, "Optical Switching: Switch Fabrics, Techniques and Architectures," IEEE J. Lightwave Technol., Vol. 21, pp. 384-405, 2003.
- [2] Y. Silberberg, P. Perlmutter, and J. E. Baran, "Digital optical switch," *Appl. Phys. Lett.*, vol. 51, pp. 1230–1232, Oct. 1987.
- [3] H. Sasaki and R. M. de la Rue, "Electro-optic y-junction modulator switch," *Electron. Lett.*, vol. 12, p. 459, 1976.
- [4] R. Hauffe, U. Seibel, J. Bruns, and K. Petermann, "Digital Optical Switches and Switching Matrices in Polymer" *Int. J. Electron. Commun.*, Vol. 55, pp. 305-312, 2001.

[5] P. Granstrand, B. Lagerström, P. Svensson, H. Olofsson, J.-E. Falk, and B. Stoltz, "Pigtailed tree-structured 8\_8 switch matrix with 112 digital optical switches," *IEEE Photon. Technol. Lett.*, Vol. 6, pp. 71–73, 1994.

[6] A. Chen, R.W. Irvin, E. J. Murphy, R. Grencavich, T. O. Murphy, and G. W. Richards, "High performance LiNbO<sub>3</sub> switches for multi wavelength optical networks," in *Proc. Photon. Switching*, pp. 113–115, July 1999.

[7] D. Hanson, "Using optical switches for facility restoration," *Lightwave*, Vol. 7, pp. 37-38, 1990.

[8] M. N. Kahn, J. E. Zucker, T. Y. Chang, N. J. Sauer, and M. D. Divino, "Weighted-coupling Y-branch optical switch in InGaAs/InGaAlAs quantum well electron transfer waveguides," *IEEE Photon. Technol. Lett.*, Vol. 6, pp. 394-397, 1994.

[9] W. K. Burns, "Shaping the digital switch," *IEEE Photon. Technol. Lett.*, Vol. 4, pp. 861–863, 1992.

[10] R. Krahenbuhl, M. M. Howerton, J. Dubinger and A. S. Greenblatt, "Performance and modeling of advanced Ti:LiNbO<sub>3</sub> digital optical switches," *IEEE J. lightwave Technol.*, Vol. 20, pp. 92-99, 2002.

[11] K. Noguchi "Ultra-High-Speed LiNbO<sub>3</sub> modulators," *Optical and Fiber Commun. Reports* Vol. 4, pp. 1-13, 2007.

[12] M. M. Howerton, R. P. Moeller, J. Dubinger, A. S. Greenblatt, and R. Krähenbühl, "Fully packaged, broad-band LiNbO<sub>3</sub> modulator with low drive voltage," *IEEE Photon. Technol. Lett.*, Vol. 12, pp. 792–794, 2000.

[13] J. Nikolopoulos and G.L. Yip, "Accurate modeling of the index profile in annealed proton exchanged LiNbO<sub>3</sub>," *Proc. SPIE, Integrated Optical Circuits*, Vol. 1583, pp. 71-82, 1991.

[14] E. Y. B. Pun, K. K. Loi, and P. S. Chung, "Experimental studies of proton-exchanged waveguides in Lithium Niobate using toluidic acid," *Proc. SPIE, Integrated Optical Circuits*, Vol. 1583, pp. 64-70, 1991.

[15] J. L. Jackel, "Proton exchange: past, present, and future," *Proc. SPIE, Integrated Optical Circuits*, Vol. 1583, pp. 54-63, 1991.

**Ghanshyam Singh** has completed B.E from REC Silchar, M.Tech from MREC Jaipur and is currently pursuing PhD. His areas of interest include Optical Communication, Optical Switches and Interconnects.

**Prof. R.P.Yadav** has completed his Master of Science and Master of Technology from IIT Delhi and Ph.D. degree from MNIT Jaipur. Presently, he is Prof. & Head ECE department, MNIT. His areas of interest are Digital and Wireless Communication and Coding, Antennas, Optics and Networking.

**Dr. Vijay Janyani** has completed B.E. and M.E. from MREC Jaipur and PhD from Nottingham University, UK. Presently, he is Associate Professor with ECE department, MNIT. His areas of interest are Optoelectronics, Nonlinear Optic and Numerical Modeling.